Effects of strain, substrate misorientation, and excitonic transition on the optical polarization of ordered zinc-blende semiconductor alloys

Yong Zhang,[a] A. Mascarenhas, P. Ernst,[b] F. A. J. M. Driessen, D. J. Friedman, K. A. Bertness, and J. M. Olson
National Renewable Energy Laboratory, Golden, Colorado 80401

C. Geng, F. Scholz, and H. Schweizer
4. Physikalisches Institut, Universtät Stuttgart, 70550 Stuttgart, Germany

(Received 22 July 1996; accepted for publication 24 January 1997)

Optical polarization in ordered $GaInP_2$ alloys has been studied by low-temperature photoluminescence. A perturbative theory that includes the effects of lattice mismatch, substrate misorientation, and excitonic transitions has been developed for making quantitative comparisons between experimental results and theoretical predictions. We show that to obtain quantitative information about ordering from the polarization of near-band-gap transitions, all of the above-mentioned effects should be taken into account. This study demonstrates that the electronic and optical properties of a monolayer superlattice formed by partial ordering in the $GaInP_2$ alloy can be well described by a simple perturbative Hamiltonian, i.e., a quasicubic model. © *1997 American Institute of Physics.* [S0021-8979(97)06209-9]

I. INTRODUCTION

It is well established that many zinc-blende semiconductors show spontaneous long-range ordering (LRO) when grown under certain conditions.[1] Various types of LRO are possible: CuPt, CuAu, and chalcopyrite. The perfectly ordered phases of these structures are one- or two-monolayer superlattices, with ordering along the [111], [001], or [201] crystallographic directions, respectively. Band-gap reductions and valence-band splittings are the common features of these ordered phases, as compared with the disordered phase. Nevertheless, each of the ordered phases shows distinct physical properties because of their differences in crystal symmetry. Although there are many sophisticated methods available for analyzing crystal symmetry, a measurement of optical polarization combined with some theoretical considerations is a relatively simple way of accomplishing this. For instance, a measurement of the polarization in the plane perpendicular to the growth direction [001] will show no anisotropy for CuAu ordering, whereas it will show anisotropy for CuPt ordering.[2]

On the other hand, the electronic structures of very-short-period superlattices (containing only a few monolayers per period) are expected to be very different from relatively large period superlattices. The latter are normally treated with the so-called envelope function approximation,[3] and it is relatively easy to compare the theoretical results of this approximation with the experimental results. For the very-short-period superlattices, because the theoretical methods are much more complex[4] and furthermore, in reality, perfectly ordered structures do not exist, a quantitative comparison between the theoretical and experimental results is less trivial.[5] To describe the electronic structure of a partially ordered alloy in an easier way, a perturbative Hamiltonian, the so-called quasicubic model,[6] has been employed.[7] This greatly simplified model uses only one parameter, the crystal-field splitting, to describe the effect of ordering on the valence band. The valence-band splitting and band-gap reduction in ordered $GaInP_2$ have been investigated optically by using a series of samples with varying degree of order.[8] It is found that the relative positions of the energy levels can be described very well by the quasicubic model.[8]

The dependence of optical polarization on the degree of order (η)[9] has been studied theoretically based on the quasicubic model and band-to-band transitions at $\mathbf{k} = 0$.[2] The effects of strain due to lattice mismatch between epilayer and substrate have been considered as well.[2] Experimentally, optical anisotropy caused by CuPt ordering has been observed in various spectroscopic studies of $GaInP_2$ alloys: photoluminescence (PL) and photoluminescence excitation (PLE),[10–12] piezomodulated reflectance,[13] reflectance difference,[14] electroreflectance,[15] photocurrent,[16] and ellipsometric measurement.[17] Qualitatively, these studies have all shown the change in crystal symmetry as a result of ordering. By applying the perturbative model of Ref. 7, the dependence of polarization on the degree of order has been used to obtain the parameter η (Ref. 2) from the electroreflectance data[15] and to explain the dependence of reflectance difference on η.[14,18] However, there has not been an independent check to the applicability of the perturbative model for describing the optical polarization. The reason for that is largely due to the constraint of sample quality. Not until recently, have high-quality ordered $GaInP_2$ samples with systematically varying ordering parameter become available.[8] By ''high-quality,'' we mean that in these samples well-identified excitonic transitions have been observed in both PL and PLE spectra.[8]

This work will focus on the optical polarization of CuPt-ordered $GaInP_2$ alloys. We (1) conduct a quantitative study on the polarization of PL as a function of η, using a set of high-quality samples; (2) study the effect of substrate mis-

[a]Electronic mail: yzhang@nrel.nrel.gov
[b]Present address: 4. Physikalisches Institut, Universtät Stuttgart, 70550 Stuttgart, Germany.

TABLE I. Samples used for studying the dependence of polarization on the degree of order (except for sample No. 5, all samples were grown under low pressure).

Sample No.	Substrate	Growth temperature (°C)	Growth rate (μm/h)	V/III ratio	Epilayer thickness (μm)	E_g (eV)
1	$6°\rightarrow[111]_A$	810	2	240	2	2.003
2	$6°\rightarrow[111]_A$	840	2	240	2	1.999
3	$6°\rightarrow[111]_B$	750	2	240	2	1.945
4	$6°\rightarrow[111]_B$	720	2	240	2	1.908
5	$6°\rightarrow[111]_B$	670	5.5	60	10	1.891
6	$6°\rightarrow[111]_B$	690	2	240	2	1.878
7	$6°\rightarrow[111]_B$	660	0.5	240	2	1.871

TABLE II. Samples used for studying the dependence of polarization on the substrate misorientation angle (except for samples in group 5, all samples were grown under atmospheric pressure).

Sample group	Substrate	Growth temperature (°C)	Growth rate (μm/h)	V/III ratio	Epilayer thickness (μm)
1	0°, 2°, 4°, and $6°\rightarrow[111]_B$	670	5.5	60	10
2	2°, 4°, 6°, and $9°\rightarrow[111]_B$	625	2	323	0.3
3	2°, 6°, and $9°\rightarrow[111]_B$	700	4.4	150	0.3
4	4° and $6°\rightarrow[111]_B$	670	5.5	60	1
5	6° and $10°\rightarrow[111]_B$	690	2	240	2

orientation on the PL polarization by using samples grown on differently tilted substrates; and (3) compare the experimental results with the perturbative model with the effects of strain, substrate misorientation, and excitonic transitions taken into account. The last two effects, which influence the quantitative analysis of the polarization measurements significantly, have not been considered in previous studies.

In Sec. II, we briefly describe the growth conditions for the samples used in this study and the experimental setup for the polarization measurement. In Sec. III, we present the experimental results. Section IV gives theoretical analyses and discussions for the effects of strain, substrate misorientation, and excitonic transitions. Section V summarizes this work.

II. SAMPLES AND EXPERIMENTAL SETUP

A. Samples

The ordered $Ga_xIn_{1-x}P$ samples were grown by low- or atmospheric-pressure metal-organic vapor-phase epitaxy (MOVPE) on GaAs substrates with various misorientation angles (ranging from 0° to 9°) toward a [111]B direction. The disordered samples were grown by low-pressure (i.e., at $P = 100$ hPa) MOVPE on GaAs substrates 6° misoriented toward [111]A. The details about sample growth are described elsewhere.[12,19] To study the dependence of polarization on the degree of order, we carefully chose a set of samples that were grown on 6°-[111]B GaAs substrates and under proper growth conditions so that large and uniform ordered domains (typically 100 nm) or well-defined η are achieved.[20] Information about these samples and the disordered ones is given in Table I. Samples used to study the dependence on the misorientation angle, listed in Table II, do not necessarily have large ordered domains; thus, the results for these samples are quantitatively less accurate, and we only used them qualitatively. In fact, optimized growth conditions have only been found for the 6° B-tilt substrate, not for other types of substrates. Thus, most of the samples in Table II were not grown at optimized conditions, so the quality is relatively poor. They may have either small or nonuniform ordered domains.[20]

All samples are single variant, except for one sample grown on a nontilted substrate. This sample contains two ordering variants with large domains ($\sim 1\ \mu$m).[19] The lattice constants of the $Ga_xIn_{1-x}P$ epilayers are nearly matched to that of GaAs at room temperature, but they have considerable deviations at liquid helium temperature because of the difference in their thermal expansion coefficients. The lattice-matched composition is $x_0 = 0.515$ and 0.520 at room temperature and liquid helium temperature, respectively. The actual compositions for the samples used in this study are in the range of $0.50 < x < 0.52$, corresponding to a range of biaxial strain $0 < |\epsilon_{\text{biaxial}}| < 0.15\%$.

B. Experimental setup

PL was excited by an argon ion laser (488 nm line), dispersed through a double grating monochrometer (Spex 1403), and detected by a GaAs-cathode photomultiplier tube (RCA C31034). The sample was mounted on the cold finger of a 10 K closed-cycle refrigerator. Assuming an untilted substrate, the polarization of the emission normal to the sample surface was measured parallel to the [110] and [110] crystalline directions. The polarization analyzer is composed of a linear polarizer and a half-wavelength retarder at 650 nm. The systematic error in determining the polarization ratio is within 1%–2% in the whole spectral range needed for this work.

III. EXPERIMENTAL RESULTS

A. Dependence of the polarization ratio on the degree of order

In this work, the ordering direction is defined along the [111] crystalline direction. The polarization ratio, R_1, is defined as the intensity ratio of the PL peak polarized parallel to the assumed [110] and [110] directions on the sample surface. These directions deviate from the true crystalline [110] and [110] directions if the sample is grown on a misoriented substrate.

Figure 1(a) shows the PL spectra of a disordered sample for two polarizations at 11 K. The weak polarization anisotropy can be understood as a result of residual ordering. In Fig. 1(b), the spectra for an ordered sample reveal a stronger polarization anisotropy for the two PL bands. The narrow band, seen only in the samples grown on substrates misoriented 6° toward [111]B under suitable conditions, is from

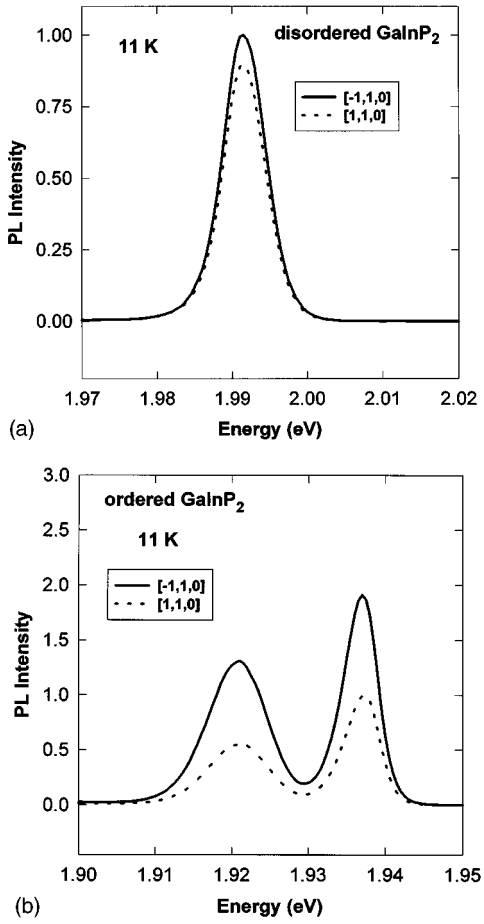

FIG. 1. Low-temperature photoluminescence of $GaInP_2$ alloys in the $[\bar{1}10]$ and [110] polarizations. (a) Disordered, and (b) ordered.

intrinsic exciton recombination,[12] the origin of the broad band, referred to as the ''moving peak,'' is uncertain, although it is expected to involve spatially indirect nonexcitonic recombination.[21,22] We will refer to the former as the high-energy peak and the latter as the low-energy peak. Our polarization measurement indicates that the hole involved in the recombination associated with the moving peak originates in an ordered region and, thus, carries the signature of the valence-band symmetry for CuPt ordering. Figure 2 is a summary of the polarization measurements for two disordered samples and a series of samples (all grown on 6°-[111]B misoriented substrates) with different degrees of ordering and, therefore, different band-gap reductions. For the ordered samples, the polarization ratios are visually independent of the degree of order. However, there is a noticeable difference between the high- and low-energy peaks. On average, the polarization ratios are about 1.9 for the high-energy peak and 2.3 for the low-energy peak in the ordered samples. These numbers significantly deviate from the ratio of 3 predicted by the model of band-to-band transitions for a CuPt-ordered alloy without strain and substrate misorientation.[2] In the next section, we will discuss how the three effects can account for the deviations (Secs. IV B–D), and the possible reason for the difference between the two peaks (Secs. IV C and D).

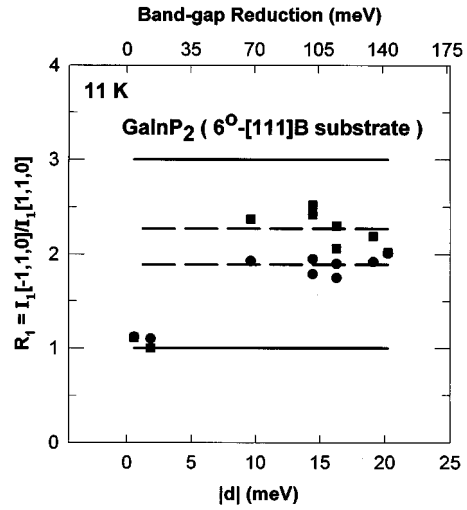

FIG. 2. Polarization ratios as a function of the degree of order. Squares and circles are for the high- and low-energy peaks in Fig. 1, respectively. Dashed lines are for the average of the experimental results. Solid lines are the theoretical predictions of the band-to-band transition model.

B. Dependence of the polarization ratio on the misorientation angle

When a tilted substrate, whose surface normal misorients from the [001] direction toward a specific direction, is used, the surface normal of the epilayer of an epitaxially grown sample also tilts to the same direction as the substrate does. The surface normal of the epilayer can differ on a microscopic scale from the surface normal of the substrate, e.g., if facets form during growth.[19] While the microscopic tilt between the substrate and epilayer facet normals can be several degrees or more, the macroscopic average epilayer surface normal will be within a small fraction of a degree of the substrate normal. A simple geometrical consideration demonstrates this. For a macroscopically flat epilayer of average thickness T grown on a substrate of lateral dimensions L, the maximum possible tilt between the epilayer and substrate normals is for the case where the epilayer is of zero thickness on one end of the substrate, increasing over the lateral distance L to $2T$ at the other end. In this case, the epilayer and surface normals differ by $\theta_0 = \arctan(2T/L)$, which is the upper limit on tilt between substrate and epilayer surface normals. For an epilayer of average thickness $T = 10\ \mu$m, grown on an $L = 1$ cm substrate, this limit is 0.1°, which is negligible for our purposes. In practice, the epilayer and substrate surface normals will be essentially identical, since adatom surface diffusion lengths limit the facet sizes to the order of microns rather than centimeters.

The effect of substrate misorientation is investigated for five groups of samples. Samples in each group were grown at the same conditions but on substrates with different misorientation angles toward the [111]B direction. The experimental results for the low-energy peak are shown in Fig. 3, where the misorientation angle dependence predicted by theory (see Sec. IV C) is shown for comparison. Indeed, the trend for samples in each group agrees with the theory, although there is scatter in the values from one group to the other. We believe that scatter in the data are mainly due to relatively

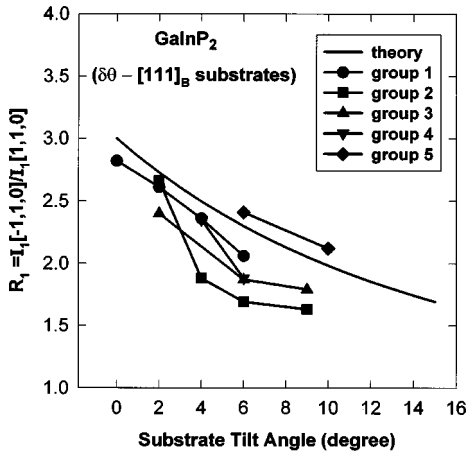

FIG. 3. Polarization ratio as a function of substrate tilt angle for $GaInP_2$ alloys grown on [111]B tilted GaAs substrates.

poor sample quality, as mentioned in the last section about sample growth. We will not make a further attempt to explain the scatter quantitatively, but will emphasize the effect of the tilt angle as an important consideration for the 6° B-tilt samples whose optical polarization will be the focus of this quantitative study.

IV. THEORETICAL ANALYSES AND DISCUSSIONS

A. Band-to-band transitions with CuPt ordering

For the band-edge states ($\mathbf{k} = 0$), ordering does not change the symmetry of the conduction-band state, but the symmetry of the valence-band states is changed. Thus, only the valence band is responsible for the change in optical transition intensities as we consider the band-to-band transitions at $\mathbf{k} = 0$. Assuming the ordering effect can be treated perturbatively, the perturbative part of the Hamiltonian can be written in the same form as for the [111] uniaxial strain:[23–25]

$$h_v = -d[(L_x L_y + L_y L_x) + \text{c.p.}], \tag{1}$$

where L is the angular momentum operator, and c.p. denotes cyclic permutation with respect to the indices x, y, and z. d is a parameter that describes the strength of the rhombohedral distortion ($|d| = \Delta_{CF}/3$, Δ_{CF} is the crystal-field-splitting parameter).[1,2] Equation (1) is in fact equivalent to the so-called quasicubic model.[6] The total Hamiltonian for the ordered alloy is $H_{ord} = H_{so} + h_v$, where H_{so} is the spin-orbit interaction for the disordered alloy. The eigenvalues of H_{ord} are given as:[6,23–25]

$$E_1 = -d, \tag{2}$$

$$E_{2,3} = -\frac{1}{2}(\Delta_{so} - d) \pm \frac{1}{2}[(\Delta_{so} + d)^2 + 8d^2]^{1/2}, \tag{3}$$

where Δ_{so} is the spin-orbit splitting of the disordered alloy, E_1 is associated with the heavy hole (HH)-like state, and E_2 and E_3 are with the light hole (LH)-like and the spin-orbit split-off states, respectively. The energy reference is assumed to be at the top of the valence band without ordering, and positive energy is toward the conduction band. Since $d < 0$ for CuPt ordering,[1,2] the topmost valence-band state is the HH-like state E_1, which is similar to the case of [111] tensile strain. Note, that Eq. (1) is given in a cubic coordinate system where x, y, and z are along the [001], [010], and [001] crystalline directions, respectively. Because in this coordinate system it is difficult to find the eigenstates of Eq. (1) analytically, the transition matrix elements were calculated numerically as a function of the degree of order in Ref. 2.

Without the coexistence of biaxial strain, it is more convenient to use a coordinate system for which z' is along the [111] ordering direction, x' and y' are in the plane perpendicular to the ordering direction: x' along the [112] and y' along the [110]. In this new coordinate system, Eq. (1) becomes

$$h_v = -d(3L_{z'}^2 - L^2). \tag{4}$$

In a basis $\{|J, m_{z'}\rangle\} = \{|3/2, -3/2\rangle, |3/2,3/2\rangle, |3/2, -1/2\rangle, |1/2, -1/2\rangle, |3/2,1/2\rangle, |1/2,1/2\rangle\}$, h_v is block diagonal. The HH-like states are purely $|3/2, \pm 3/2\rangle$, the LH-like states, as well as the split-off states, are mixtures of $|3/2, -1/2\rangle$ and $|1/2, -1/2\rangle$ or $|3/2,1/2\rangle$ and $|1/2,1/2\rangle$. The eigenstates are: $U_1 = |3/2, -3/2\rangle$ and $U_2 = |3/2,3/2\rangle$ for the HH-like states, $U_3 = a_1|3/2, -1/2\rangle + a_2|1/2, -1/2\rangle$ and $U_4 = a_1|3/2,1/2\rangle + a_2|1/2,1/2\rangle$ for the LH-like states, $U_5 = b_1|3/2, -1/2\rangle + b_2|1/2, -1/2\rangle$ and $U_6 = b_1|3/2,1/2\rangle + b_2|1/2,1/2\rangle$ for the split-off states, where $a_1 = (E_3 + d)/\sqrt{(E_3+d)^2 + 2d^2}$, $a_2 = -\sqrt{2}d/\sqrt{(E_3+d)^2 + 2d^2}$, $b_1 = (E_2 + d)/\sqrt{(E_2+d)^2 + 2d^2}$, and $b_2 = -\sqrt{2}d/\sqrt{(E_2+d)^2 + 2d^2}$. The transition intensity, which is proportional to the square of the transition matrix element, can be given analytically for each band-to-band transition (summed over the degenerate states):

$$I_1 = e_1^2 + e_2^2 \tag{5}$$

for the transitions between the HH-like states and the conduction-band states (HH-CB),

$$I_2 = \frac{2a_2^2}{3} + \frac{(a_1^2 + 2\sqrt{2}a_1a_2)}{3}(e_1^2 + e_2^2) + \frac{4(a_1^2 - \sqrt{2}a_1a_2)}{3} e_3^2 \tag{6}$$

for the transitions between the LH-like states and the conduction-band states (LH–CB), and

$$I_3 = \frac{2b_2^2}{3} + \frac{(b_1^2 + 2\sqrt{2}b_1b_2)}{3}(e_1^2 + e_2^2) + \frac{4(b_1^2 - \sqrt{2}b_1b_2)}{3} e_3^2 \tag{7}$$

for the transitions between the split-off states and the conduction-band states (SO–CB), where $\mathbf{e} = (e_1, e_2, e_3)$ is a unit vector in the direction of the polarization of the light in the (x', y', z') coordinate system. Note that $I_1 + I_2 + I_3 = 2$. Another advantage of choosing the [111] direction as the quantization axis is that the transition intensity for any state and direction is a continuous function of the degree of order. If the [001] direction was chosen as the quantization axis, we would have a discontinuous change in the transition intensity for certain polarization directions when the ordering pertur-

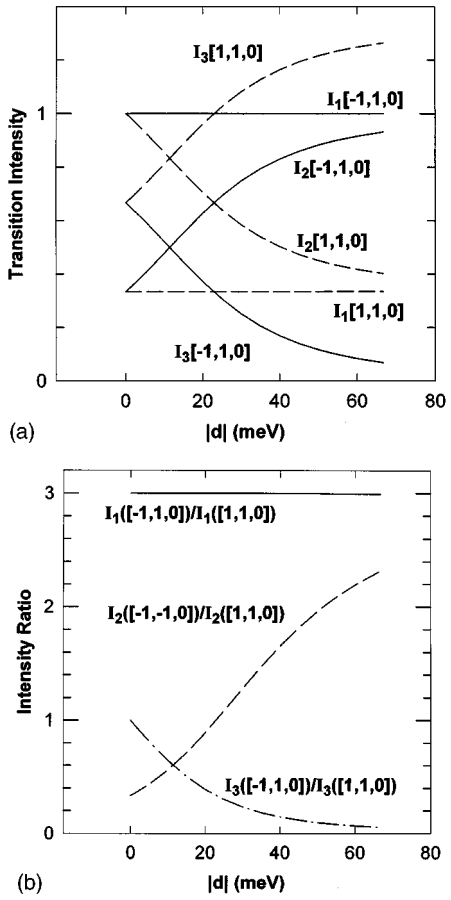

FIG. 4. Calculated transition intensities (a) and intensity ratios (b) using the band-to-band transition model as a function of crystal-field splitting parameter d for [110] and [110] polarizations.

bation was turned on and off. For instance, the transition intensity of the HH–CB transition exchanges between the [111] and [001] directions because the preferred axis changes from the [001] to [111] as the ordering is turned on.

As one can see, the HH–CB transition intensity, I_1 of Eq. (5), is independent of the degree of order. The HH–CB transition can be understood as the radiation of a dipole along the z' direction. It is then easy to get the polarization ratio between the [110] and [110] directions: [110] is in the $x'-y'$ plane, and [110] is out of the plane by an angle $\theta = \arccos(1/\sqrt{3})$; thus $R_1 = I_1([110])/I_1([110]) = [\cos(\theta)]^{-2} = 3$. Both the LH–CB and SO–CB transitions rather strongly depend on the degree of order. Figures 4(a) and 4(b) show the three transition intensities and the related intensity ratios for the [110] and [110] polarizations as functions of $|d|$ which reflects the degree of order.[25] Note that in the disordered limit, E_1 and E_2 are degenerate, and the combined ratio is isotropic as expected.

Because the ratio R_1 of the HH–CB transition is independent of the degree of order, this property can be exploited to examine other possible mechanisms that may cause the discrepancy between experimental results and the theoretical predictions. On the other hand, the polarization ratios for the LH–CB transition, $R_2 = I_2([110])/I_2([110])$, and the SO–CB transition, $R_3 = I_3([110])/I_3([110])$, strongly depend on the degree of order. In principle, such a dependence can be used to measure the degree of order, as in Ref. 2 where the polarization dependence of the LH–CB transition is used to obtained the degree of order. Nevertheless, to do so, various corrections are necessary as will be discussed in the following subsections.

B. Strain effect due to lattice mismatch

The strain effect in ordered $GaInP_2$ has been studied by a few groups.[2,26,27] The strain Hamiltonian can be written as[23,24]

$$h_s = a_v(\epsilon_{xx}+\epsilon_{yy}+\epsilon_{zz}) - 3b_v[(L_x^2 - L^2/3)\epsilon_{xx} + \text{c.p.}], \quad (8)$$

in the cubic coordinate system, where a_v and b_v are the hydrostatic and shear deformation potentials for the valence band, respectively, and ϵ_{ii} are the diagonal components of the strain tensor $\epsilon = \epsilon_{xx} = \epsilon_{yy} = (a_{\text{sub}} - a_{\text{epi}})/a_{\text{sub}}$, $\epsilon_{zz} = -(2C_{12}/C_{11})\epsilon$, where a_{sub} and a_{epi} are the lattice constants of the substrate and the epilayer, respectively, and C_{ij} are the elastic constants. For a $Ga_xIn_{1-x}P$ epilayer, when $x < x_0 (x > x_0)$, the epilayer is subject to a biaxially compressive (tensile) strain. In both cases, the strain effect tends to enhance the HH–LH splitting.[2] The situation of biaxially

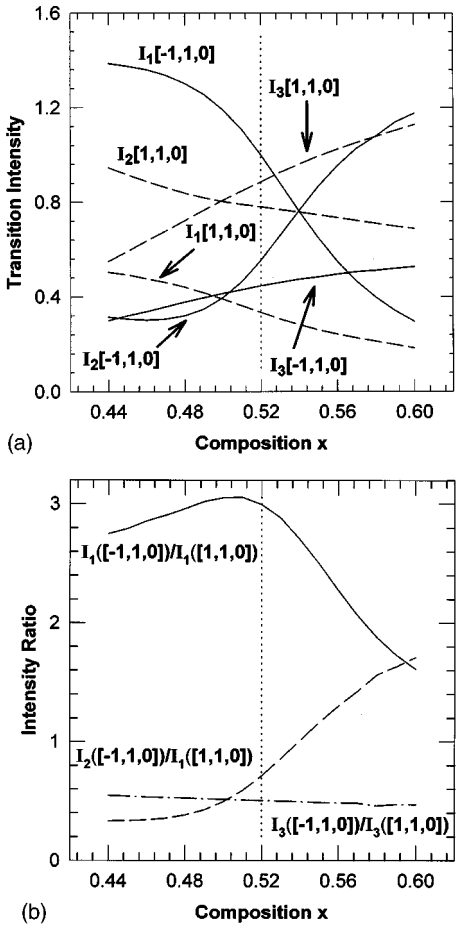

FIG. 5. Calculated transition intensities (a) and intensity ratios (b) using the band-to-band transition model as a function of Ga composition between different polarizations, with the strain effect considered. Vertical line indicates the lattice-matched composition.

TABLE III. Parameters for $Ga_xIn_{1-x}P$ alloys.

$E_g = 2.884x + 1.424(1-x) - 0.76x(1-x)$ (eV)
$\Delta_{so} = 0.080x + 0.110(1-x) + 0.035x(1-x)$ (eV)
$\gamma_1 = 4.05x + 5.05(1-x)$
$\gamma_2 = 0.49x + 1.6(1-x)$
$\gamma_3 = 1.25x + 1.73(1-x)$
$E_p = 31.4x + 20.7(1-x)$ (eV)
$a_{epi} = 5.4470x + 5.8658(1-x)$ (Å)
$a_{GaAs} = 5.6480$ (Å)
$a_c - a_v = -9.3x - 6.6(1-x)$ (eV)
$b_v = -1.4x - 1.55(1-x)$ (eV)
$C_{11} = 143.87x + 106.9(1-x)$ (GPa)
$C_{12} = 65.20x + 61.1(1-x)$ (GPa)

compressive strain frequently occurs when one intends to grow samples lattice matched to the GaAs substrate at room temperature.

With the coexistence of CuPt ordering and biaxial strain, neither [001] nor [111] is a preferred quantization axis. Simple analytic solutions are impossible in this situation. We calculate the transition intensities numerically in the same way as that in Ref. 2, where the matrix form of Eq. (8) is taken from Ref. 28. The strain effect is shown in Figs. 5(a) and 5(b) for the intensity and the intensity ratios, respectively, for the [110] and [$\bar{1}$10] polarizations. Note that with the coexistence of ordering and strain, the HH–CB transition becomes dependent on the degree of order. A typical value of $d = -15$ meV ($\eta = 0.47$), corresponding to a valence-band splitting of 25 meV, has been assumed. The parameters used in our calculation are listed in Table III.

One can see from Fig. 5(a) that for the HH–CB transition the biaxially compressive strain ($x < x_0$) enhances the transition intensities of the [110] and [$\bar{1}$10] polarizations, as has been pointed in Ref. 26. On the other hand, the biaxially tensile strain ($x > x_0$) has an opposite effect on these polarization directions. For the intensity ratios, R_1 of the HH–CB transition has a very weak strain dependence in the composition range $0.50 < x < 0.52$ ($|\delta R_1/R_1| < 2\%$); however, R_2 of the LH–CB transition shows a stronger strain dependence $|\delta R_2/R_2|$ can be as large as 30% in the same composition range, which corresponds to underestimating η by 30% if R_2 is used to determine the degree of order without considering the strain effect. For the intensity ratio of the HH–CB transition, shown in Fig. 2, the strain effect is insignificant.

C. Effect of substrate misorientation

When the substrate is tilted toward one of the three directions [111]A, [111]B, or (110)AB (a direction between the other two), by an angle $\delta\theta$, the apparent [110] and [$\bar{1}$10] directions, denoted as the $[110]_a$ and $[\bar{1}10]_a$ directions, with respect to the sample surface may not be the true [110] and [$\bar{1}$10] crystalline directions. Thus, the measured polarization ratio cannot be compared directly with that shown in Fig. 4(b). For the [111]B tilted substrate, the $[\bar{1}10]_a$ direction coincides with the [110] direction, but the $[110]_a$ direction corresponds to the $[\cos(\delta\theta), \cos(\delta\theta), -\sqrt{2}\sin(\delta\theta)]$ direction. In general, assuming the substrate is tilted by an angle $\delta\theta$ toward a direction in the x-y plane with an azimuth angle φ from the x axis, the transformation between $[x,y,z]$ and $[x_1,y_1,z_1]_B$ is given as

$$\begin{pmatrix} x \\ y \\ z \end{pmatrix} = \begin{pmatrix} \cos(\delta\theta)\cos^2\varphi + \sin^2\varphi & [\cos(\delta\theta)-1]\cos\varphi\sin\varphi & \sin(\delta\theta)\cos\varphi \\ [\cos(\delta\theta)-1]\cos\varphi\sin\varphi & \cos(\delta\theta)\sin^2\varphi + \cos^2\varphi & \sin(\delta\theta)\sin\varphi \\ -\sin(\delta\theta)\cos\varphi & -\sin(\delta\theta)\sin\varphi & \cos\delta\theta \end{pmatrix} \begin{pmatrix} x_1 \\ y_1 \\ z_1 \end{pmatrix}. \tag{9}$$

Here φ=45°, 90°, and 135° correspond to a [111]B, (110)AB, and [111]A tilted substrate, respectively.

For the HH–CB transition, the polarization ratio R_1 between the $[\bar{1}10]_a$ and $[110]_a$ directions can be calculated for the three tilted directions as follows:

$$R_1^{[111]A} = 3\left(1 - \frac{1}{3}\sin^2(\delta\theta)\right) \tag{10}$$

for the [111]A misorientation;

$$R_1^{[111]B} = \frac{3}{1 + \sqrt{2}\,\sin(2\delta\theta) + \sin^2(\delta\theta)} \tag{11}$$

for the [111]B misorientation; and

$$R_1^{(110)AB} = \frac{2 + \cos(\delta\theta) - \sin(\delta\theta) + \frac{1}{2}\sin(2\delta\theta)}{2 - \cos(\delta\theta) + \sin(\delta\theta) + \frac{1}{2}\sin(2\delta\theta)} \tag{12}$$

for the (110)AB misorientation. All three equations yield a limit value of 3 as $\delta\theta \to 0$.

The calculated $\delta\theta$ dependence for the [111]B misorientation is shown in Fig. 3. For a typical value of $\delta\theta = +6°$, we have $R_1^{[111]A} = 2.995$, $R_1^{[111]B} = 2.30$, and $R_1^{(110)AB} = 2.47$. Note that the sign of $\delta\theta$ is very meaningful. That experimentally observed $R_1^{[111]B} < 3$ or $\delta\theta > 0$ allows us to unambiguously identify along which of the two equivalent [111]B directions is the ordering axis. In fact, this direction agrees with that obtained from the surface step ordering model.[29] If the ordering were along the other direction, that is, $\delta\theta < 0$, one would have observed $R_1^{[111]B} > 3$ (for instance, if $\delta\theta = -6°$, $R_1^{[111]B} = 4.20$). The strong $\delta\theta$ dependence comes

from the fact that in the plane that contains the [111] and [110] directions the transition intensity varies rapidly from zero for the polarization along the [111] (z') direction to a maximum along the [112] (x') direction according to the dependence on $\cos^2(\theta)$ as mentioned in Sec. IV A.

Note that the calculated ratio $R_1 = 2.30$ for the $6° - [111]$B misorientation is the same as that measured for the low-energy peak shown in Fig. 2, which is supportive of its assignment as a nonexcitonic or band-to-band transition made in Ref. 22. For the high-energy peak, the effect of substrate misorientation has partially accounted for the deviation between the experimental results and the band-to-band transition model. The exciton effect, discussed in the next subsection, is primarily responsible for the difference between the high- and low-energy peaks.

In general, the effect of the tilted substrate is relatively weak for the LH–CB and SO–CB transitions. For instance, considering a $6° - [111]$B sample with $|d| = 15$ meV, we get $|\delta R_2/R_2| = 4.3\%$ for the LH–CB transition (which corresponds to overestimating η by 3% if R_2 is used to determine the degree of order without considering the substrate misorientation), and $|\delta R_3/R_3| = 8.4\%$ for the SO–CB transition, compared with $|\delta R_1/R_1| = 23.3\%$ for the HH–CB transition.

D. Excitonic transitions

It is obvious that the band-to-band transition theory cannot produce the excitonic features[12] in the absorption or PLE spectrum. However, in this work, we are mainly interested in the polarization of the band-edge transitions, i.e., excitonic transitions at $\mathbf{k}_{ex} = 0$ ($\mathbf{k}_{ex}$ is the wave vector of the excitonic state). Thus, we would like to know how significantly the formation of excitons can affect the polarization of the band-edge transitions. The optical transition matrix element for an excitonic state at $\mathbf{k}_{ex} = 0$ is given by:[30,31]

$$M_{ex}(k_{ex}=0) = \sum_{\mathbf{k}} A(\mathbf{k}) M_{cv}(\mathbf{k}), \tag{13}$$

where $M_{cv}(\mathbf{k}) = \langle \varphi_c(\mathbf{k}) | \mathbf{e}\cdot\mathbf{p} | \varphi_v(\mathbf{k}) \rangle$ is the matrix element for the direct band-to-band transition, $\mathbf{p}$ is the momentum operator, and $A(\mathbf{k}) = \Sigma_k \exp(-i\mathbf{k}\cdot\mathbf{x}) F_1(\mathbf{x})$ is the Fourier transform of the ground-state exciton wave function $F_1(\mathbf{x})$. $A(\mathbf{k})$ is usually localized at $\mathbf{k} = 0$, which is the justification for the effective mass approximation. If we assume that $\mathbf{M}_{cv}(\mathbf{k})$ is a smooth function of $\mathbf{k}$, then $|M_{ex}(k_{ex}=0)|^2 \approx |M_{cv}(0)|^2 |F_1(0)|^2$, that is the polarization of an excitonic transition is the same as that of the band-to-band transition at $\mathbf{k} = 0$. Nevertheless, in general, the polarization of an excitonic transition is different from that of the related band-to-band transition at $k = 0$, because of the involvement of the $\mathbf{k} \neq 0$ states in the excitonic transition. Since in the band-to-band transition model, we have $R_1 > R_2$ for the two polarization ratios of most interest in experiments, we expect that the excitonic effect will cause a decrease in R_1 and an increase in R_2 because of the mixing of wave functions for $\mathbf{k} \neq 0$ states. There are two situations where we cannot apply this approximation: (1) $M_{cv}(\mathbf{k})$ changes significantly in the $\mathbf{k}$ region where $A(\mathbf{k})$ is not negligibly small; and (2) for certain polarization $M_{cv}(0) = 0$; for instance, along the ordering direction [111] the HH–CB transition is forbidden according to the band-to-band transition theory. If the excitonic effect is taken into account, the transition becomes partially allowed. A similar effect appears for some forbidden transitions in the [001] grown superlattices.[31]

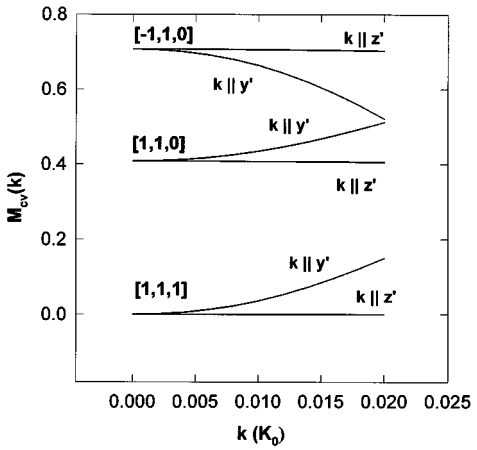

FIG. 6. Transition matrix element $M_{cv}(\mathbf{k})$ for the HH-CB transition as a function of $\mathbf{k}$ for different polarizations.

The matrix element $M_{cv}(\mathbf{k})$ is calculated by an eight-band $\mathbf{k}.\mathbf{p}$ model.[25] Figure 6 shows the $M_{cv}(\mathbf{k})$ of the HH–CB transitions for $\mathbf{k}$ parallel to the y' and z' directions for a few typical polarizations. Note that even for $\mathbf{k}$ in the plane perpendicular to the ordering direction, $M_{cv}(\mathbf{k})$ is anisotropic and strongly depends on the relative orientation between the $\mathbf{k}$ and $\mathbf{e}$. However, in the ($x'y'z'$) coordinate system, $A(\mathbf{k})$ is not a function of the azimuth angle, so one can average $M_{cv}(\mathbf{k})$ over the azimuth angle when evaluating Eq. (13).

As has been shown previously, the CuPt ordered $GaInP_2$ has an ellipsoidal band structure near $\mathbf{k} = 0$.[25] Within the effective mass approximation, the exciton wave function can be written in the form of[32]

$$F_1(\mathbf{x}) = (a^2 b \pi)^{-1/2} \exp(-\sqrt{(x^2+y^2)/a^2 + z^2/b^2}), \tag{14}$$

the exciton binding energy and parameters a and b are obtained variationally with the above trial wave function. $A(\mathbf{k})$ is indeed fairly localized in $\mathbf{k}$ space [$A(0.02K_0)/A(0) < 0.05$, $K_0 = 2\pi/a_0$, and a_0 is the lattice constant], which ensures the validity of the effective mass approximation.

With the obtained $M_{cv}(\mathbf{k})$ and $A(\mathbf{k})$, the matrix element $M_{ex}(\mathbf{k}_{ex} = 0)$ for the excitonic transition has been calculated according to Eq. (13). As an example, assuming a typical degree of order with $|d| = 15$ meV, the polarization ratios for the excitonic transitions is $R_1 = 2.80$ for the HH–CB transition, compared to 3 from the band-to-band transition model. Although in Fig. 6 $M_{cv}(\mathbf{k})$ shows a rather strong $\mathbf{k}$ dependence in certain $\mathbf{k}$ directions, after averaging over $\mathbf{k}$ space, the effect becomes less significant. However, it is a detectable effect. By including the excitonic effect, the transition intensity as well as the polarization ratio become η dependent. We expect that the polarization ratio R_1 decreases as the HH–LH mixing increases with decreasing the degree of order. For instance, $R_1 = 2.66$ for $|d| = 10$ meV($\eta = 0.39$)

TABLE IV. Effects of substrate misorientation and excitonic transitions on the polarization ratios.

		$I([\bar{1}10])/I([110])$	$I([110])/I([111])$
0°	band–band	3.00	∞
	exciton	2.80	14
6°[111]B	band–band	2.30	40
	exciton	2.20	11

and $R_1 = 2.99$ for $|d| = 67$ meV($\eta = 1$). An important excitonic effect is that the HH–CB transition for the [111] polarization becomes allowed, though its intensity is still more than one order of magnitude weaker than that of the [110] polarization. For instance, for $|d| = 15$ meV, the ratio $I_1([110])/I_1([111]) = 14$. Furthermore, for the case of a 6° [111]B misoriented substrate and $|d| = 15$ meV, the polarization ratio R_1 for the HH–CB transition becomes 2.20 with the excitonic effect taken into account. For $|d| = 10$ meV, R_1 reduces to 2.1. On the other hand, the excitonic effect for the LH–CB transition is relatively weak, compared to the HH–CB transition.

Table IV summarizes the effects of the substrate misorientation and the excitonic transition for the HH–CB transition with $|d| = 15$ meV. The value of 2.20 for R_1 is in reasonably good agreement with the experimental result shown in Fig. 2, which gives a somewhat lower average value of 1.9. One possible reason for the deviation is that the exciton localization due to various fluctuations (compositions, degree of order, domain size, and short-range ordering[33]) could cause stronger HH–LH mixing, and consequently a lower ratio R_1. It is also possible that our model for calculating the exciton states is oversimplified. Roughly speaking, the ellipsoidal dispersions are accurate only within a range of $|\mathbf{k}| < k_0$ corresponding to an energy range comparable to $|d|$ above the $\mathbf{k} = 0$ states. The $\mathbf{k} \neq 0$ states that contribute significantly to the excitonic transition are in a range of $k_s \sim 2\pi/a$ or $2\pi/b$. For the ellipsoidal dispersion to be a good approximation, we have assumed $k_s < k_0$ or the HH–LH splitting to be significantly larger than the exciton binding energy. However, for the currently available samples, this condition is not always well satisfied (for $|d| = 15$ meV, the HH–LH splitting is 25 meV and the exciton binding energy is about 6 meV[8]). A more rigorous treatment for the exciton states would be a six-band model,[34] which is expected to yield stronger HH–LH coupling, thus lower ratio R_1, especially for relatively weak ordering.

Also, we have ignored the effect of the exchange interaction.[24,35] Briefly, the exchange interaction greatly affect the transition intensity when the ordering is very weak, i.e., in the cases of $|d| \sim J$, where J is the exchange interaction constant (typically $J < 1$ meV). When the ordering effect is relatively strong such that $|d| \gg J$, the exchange interaction mainly causes a splitting of the exciton state derived from the LH state with a splitting $\sim J$. The low and high energy states are dipole allowed for the polarization perpendicular and parallel to the ordering direction, respectively.[36]

E. Discussions

According to the above analyses, for the frequently measured polarization ratios between the [110] and [110] directions, the strain effect for the HH–CB transition is weak when $x < x_0$, strong when $x > x_0$, and strong for the LH–CB transition; the effect of the substrate misorientation is strong for the HH–CB transition but weak for the LH–CB transition; finally the excitonic effect is significant for the HH–CB transition but weak for the LH–CB transition. Thus, if the strain due to the lattice mismatch can be avoided, the polarization dependence of the LH–CB transition will be the best candidate for probing the degree of order by absorption or luminescence measurements.

On the other hand, in photoreflectance related measurements[13–15,17] both the real and imaginary parts of the dielectric function contribute to the measured properties. In the vicinity of the band-gap energy, the imaginary part of the dielectric constant is mainly determined by the properties (transition matrix element, reduced masses, etc.) at the band gap, but the real part of the dielectric constant is associated to the relevant properties of all the nearby bands.[37] For the polarization difference of the photoreflectance near the band-gap energy E_g, the major contribution is from the difference in the real part.[14,18] Thus, reflectance difference is related to not only the transition intensity I_1 but also the transition intensities I_2 and I_3. If reflectance related techniques are to be used for probing the degree of order,[2,14,18] all three effects: strain, substrate misorientation and excitonic transition, must be accounted for simultaneously.

V. SUMMARY AND CONCLUSIONS

We have performed a quantitative investigation of the optical polarization in CuPt-ordered zinc-blende semiconductors, both experimentally and theoretically. Within experimental uncertainty, the polarization ratio of the HH–CB transition is independent of the degree of order, although the theory predicts a weak dependence. The experimental result can be described fairly well by the quasicubic model. Analytical formulas are given for calculating transition matrix elements with arbitrary polarization and degree of order. In general, to obtain quantitative information about ordering from optical polarization measurements, the following effects should be considered: (1) strain caused by lattice mismatch, (2) substrate misorientation, (3) excitonic transition.

ACKNOWLEDGMENTS

We are very grateful to Dr. A. Zunger, Dr. S.-H. Wei, Dr. S. Froyen, Dr. S. B. Zhang, Dr. L. W. Wang, and Dr. Lok C. Lew Yan Voon for valuable discussions and suggestions. This work was supported by the Office of Energy Research, Material Science Division of the DOE under Contract No. DE-AC36-83CH10093.

[1] A. Zunger and S. Mahajan, in *Handbook on Semiconductors*, 2nd ed., edited by S. Mahajan (Elsevier, Amsterdam, 1994), Vol. 3, Chap. 19, p. 1399.
[2] S.-H. Wei and A. Zunger, Phys. Rev. B **49**, 14337 (1994).
[3] G. Bastard, *Wave Mechanics Applied to Semiconductor Heterostructures* (Les Editions de Physique, Les Ulies, 1988).

[4] L. J. Sham and Y. T. Lu, J. Lumin. **44**, 207 (1990).
[5] W.-K. Ge, W. D. Schmidt, M. D. Sturge, L. N. Pfeiffer, and W. W. West, J. Lumin. **59**, 163 (1994).
[6] J. J. Hopfield, J. Chem. Solids **15**, 97 (1960).
[7] S.-H. Wei, D. B. Laks, and A. Zunger, Appl. Phys. Lett. **62**, 1937 (1993).
[8] P. Ernst, C. Geng, F. Scholz, H. Schweizer, Y. Zhang, and A. Mascarenhas, Appl. Phys. Lett. **67**, 2347 (1995).
[9] D. B. Laks, S.-H. Wei, and A. Zunger, Phys. Rev. Lett. **69**, 3766 (1992).
[10] G. S. Horner, A. Mascarenhas, R. G. Alonso, D. J. Friedman, K. Sinha, K. A. Bertness, J. G. Zhu, and J. M. Olson, Phys. Rev. B **48**, 4944 (1993).
[11] G. S. Horner, A. Mascarenhas, R. G. Alonso, S. Froyen, K. A. Bertness, and J. M. Olson, Phys. Rev. B **49**, 1727 (1994).
[12] P. Ernst, C. Geng, F. Scholz, and H. Schweizer, Phys. Status Solidi B **193**, 213 (1995).
[13] R. G. Alonso, A. Mascarenhas, G. S. Horner, K. A. Bertness, S. R. Kurtz, and J. M. Olson, Phys. Rev. B **48**, 11833 (1993).
[14] J. S. Luo, J. M. Olson, K. A. Bertness, M. E. Raikh, and E. V. Tsiper, J. Vac. Sci. Technol. B **12**, 2552 (1994).
[15] T. Kanata, M. Nishimoto, H. Nakayama, and T. Nishino, Appl. Phys. Lett. **63**, 512 (1993).
[16] T. Kita, A. Fujiwara, H. Nakayama, and T. Nishino, Appl. Phys. Lett. **66**, 1794 (1995).
[17] F. Alsina, M. Garriga, M. I. Alonso, J. Pascual, J. Camassel, and R. W. Glew, in *Physics of Semiconductors-Proceedings of the 22nd International Conference Vancouver, Canada, 1994*, edited by D. J. Lockwood (World Scientific, Singapore, 1995), p. 253.
[18] S.-H. Wei and A. Zunger, Phys. Rev. B **51**, 14110 (1995).
[19] D. J. Friedman, G. S. Horner, S. R. Kurtz, K. A. Bertness, J. M. Olson, and J. Moreland, Appl. Phys. Lett. **65**, 878 (1994).
[20] P. Ernst, C. Geng, G. Hahn, F. Scholz, H. Schweizer, F. Phillipe, and A. Mascarenhas, J. Appl. Phys. **79**, 2633 (1996).
[21] M. C. Delong, W. D. Ohlsen, I. Viohl, P. C. Taylor, and J. M. Olson, J. Appl. Phys. **70**, 2780 (1991).
[22] E. D. Jones, D. M. Follstaedt, H. Lee, J. S. Nelson, R. P. Schneider, Jr., R. G. Alonso, G. S. Horner, J. Machol, and A. Mascarenhas, in *Physics of Semiconductors–Proceedings of the 22nd International Conference*, Vancouver, Canada, 1994, edited by D. J. Lockwood (World Scientific, Singapore, 1995), p. 293.
[23] G. L. Bir and G. E. Pikus, *Symmetry and Strain-Induced Effects in Semiconductors* (Wiley, New York, 1974).
[24] F. Pollak, Surf. Sci. **37**, 863 (1973).
[25] Y. Zhang and A. Mascarenhas, Phys. Rev. B **51**, 13162 (1995).
[26] Y. Ueno, Appl. Phys. Lett. **62**, 553 (1993).
[27] G. G. Forstmann, F. Barth, H. Schweizer, M. Moser, C. Geng, F. Scholz, and E. P. O'Reilly, Semicond. Sci. Technol. **9**, 1268 (1994).
[28] Y. Zhang, Phys. Rev. B **49**, 14352 (1994).
[29] T. Suzuki and A. Gomyo, in *NATO ASI Series, Physical Properties of Semiconductor Interfaces at Subnanometer Scale*, edited by H. W. Salemink (Kluwer, Dordrecht, 1993).
[30] F. Bassani and G. P. Parravicini, *Electronic States and Optical Transitions in Solids* (Pergamon, Oxford, 1975), p. 190.
[31] Y. C. Chang and J. N. Schulman, Phys. Rev. B **31**, 2069 (1985).
[32] W. Kohn and J. M. Luttinger, Phys. Rev. **98**, 915 (1955).
[33] K. A. Mäder and A. Zunger, Phys. Rev. B **51**, 10462 (1995).
[34] A. Baldereschi and N. O. Lipari, Phys. Rev. B **3**, 439 (1971).
[35] D. W. Langer, R. N. Euwema, K. Era, and T. Koda, Phys. Rev. B **2**, 4005 (1970).
[36] Y. Zhang and A. Mascarenhas (unpublished).
[37] J. Callaway, *Quantum Theory of the Solid State*, 2nd ed. (Academic, San Diego, 1991), p. 567.